Effect of support sinusoidal motions on the vibration of an on-board rotor-bearing system

M. Zaki Dakel, Sébastien Baguet, Régis Dufour

XVIIIth symposium
Vibrations, Chocs et Bruit* & ASTELAB
*VISHNO (VIbrations, SHocks & NOise)
July 3, 4 and 5, 2012
Centre de recherche EDF
de Clamart

Vibrations, Shocks and Noise

Effect of support sinusoidal motions on the vibration of an on-board rotor-bearing system

Mzaki Dakel, Sébastien Baguet*, Régis Dufour

Université de Lyon, CNRS, INSA-Lyon, LaMCoS UMR5259, F-69621, France

Abstract

In generator and pump rotors installed in power plants, the rotating mass unbalance and the different motions of the rotor support are among the main sources of flexural vibrations. This work aims to observe the dynamic behavior of an on-board rotor subject to rigid support movements. The modeling takes into account six types of support deterministic motions (rotational and translational motions) when the kinetic and strain energies in addition to the virtual work of the rotating flexible rotor components are calculated. The finite element method is applied using the Timoshenko beam theory. The proposed on-board rotor model considers the rotary inertia, the gyroscopic inertia, the shear deformation of shaft as well as the geometric asymmetry of shaft and/or rigid disk of the rotor. By computing the Rayleigh damping coefficients, the effect of rotor internal damping is included in the study. The Lagrange's equations are used to obtain the differential equations of the rotor in bending relative to the rigid support which forms a noninertial reference frame. The equations of motion exhibit periodic parametric coefficients due to the asymmetry of the rotor and time-varying parametric coefficients due to the support rotations. In the presented applications, the rotor mounted on rigid/elastic linear bearings is excited by a rotating mass unbalance combined with sinusoidal oscillations of the rigid support. The dynamic behavior of the rotor is analyzed by means of rotor orbits and fast Fourier transforms (FFTs).

Keywords: Rotordynamics, asymmetric rotor, on-board rotor, finite element method, elastic bearing, support motion, parametric excitation.

1. Introduction

Many industrial applications include rotating machines in which the rotor plays a dominant role. There are many studies concerning the prediction of dynamics of rotor systems mounted on elastic bearings in the case of fixed support [1,2]. Some studies observed the instability of systems subjected to parametric excitations [3]. Kang et al. [4] employed the Timoshenko beam finite elements for modeling asymmetric rotor-bearing systems. Some other works concentrated on the behavior of a rotor under the seismic excitations [5-7]. Subbiah et al. [8] studied the response of rotor systems under random support excitations using modal analysis methods. Lee et al. [9] focused on the experimental behavior of a rotor under support shock excitation. Da Silva Tuckmantel et al. [10] represented the supporting structure (foundation) of a rotating system by coupled as well as uncoupled modes for calculating the system response. In [11], experimental tests have been shown for a flexibly supported undamped rigid block foundation in rotating machinery. Duchemin et al. [12] observed the stability of a simple rotor model under a support sinusoidal rotation. Driot et al. [13] described the orbits of a rotor induced by a support harmonic rotational movement. El-Saeidy and Sticher [14] obtained the responses of a rigid rotor-bearing system subjected to rotating

* Corresponding author. Tel.: +33 4 72 43 81 93; fax: +33 4 78 89 09 80.
E-mail address: sebastien.baguet@insa-lyon.fr (S. Baguet).

mass unbalance plus support harmonic excitations. Das et al. [15] investigated the active vibration control of a flexible rotor system excited by mass unbalance and periodic rotational motion of the support. Among all the literature mentioned above, there are references studying support-excited rotor systems and whose few works dealt with the harmonically excited on-board rotors [12-15]. Moreover, these references concentrated on the investigation of dynamic behavior of either simple rotors or rotors supported by elastic bearings with constant damping and stiffness coefficients or rotors excited by support simple motions. As a consequence, the applications proposed in these works are not suitable for realistic ones. In this paper, an improved model is presented. Namely, an asymmetric rotor is discretized using the finite element method based on the Timoshenko beam theory, mounted on hydrodynamic bearings linearized with damping and stiffness coefficients calculated using the Reynolds equation [16], and excited by different motions of its support. The rotary and gyroscopic inertias, shaft shear deformation and rotor geometric asymmetry are taken into account. The linear equations of motion point out periodic parametric terms due to the rotor geometric asymmetry and time-varying parametric terms due to the support rotational excitations. In the presented examples, the rotor mounted on rigid or elastic linear bearings is subjected to rotating mass unbalance combined with support sinusoidal rotational motions. Numerical solutions are computed and analyzed by means of orbits of the rotor as well as fast Fourier transforms (FFTs).

2. Preliminary calculations

Three principal frames of reference shown in Fig. 1a are introduced to take into consideration the movement of the rotor rigid support. They are linked with the ground R^g, the rigid support R and the moving rotor R^l.

The rotational motions of the rotor support are defined by the angular velocity vector components ω^x, ω^y and ω^z of the rigid support R with respect to the ground R^g projected in the frame R. The translational motions of the rotor support are defined by the coordinates x_O, y_O and z_O of the position vector $\mathbf{O^gO}$ expressed in the frame attached to the support R. The Euler angles ψ, θ and ϕ (see Fig. 1b) allow defining the orientation of the rotor R^l with respect to its support R. The angular velocity vector of the rotor R^l with respect to the ground R^g measured in the frame R^l is defined by [12]:

$$\boldsymbol{\omega}_{R^l}^{R^g} = \boldsymbol{\omega}_{R^l}^{R} + \boldsymbol{\omega}_{R}^{R^g} = \left\langle \omega^{x^l}, \omega^{y^l}, \omega^{z^l} \right\rangle_{R^l}^{T} \qquad (1)$$

where T is a matrix transpose. The components (ω^{x^l}, ω^{y^l}, ω^{z^l}) are formulated as a function of (ψ,θ,ϕ) and their time derivative as well as ($\omega^x,\omega^y,\omega^z$). The rotor is supposed to rotate at a constant speed Ω. So the spinning angle ϕ is replaced by Ωt and its derivative $\dot{\phi}$ by Ω ($\bullet$ denotes differentiation with respect to time t). Let us consider a generic point C^0 along the elastic line of the nondeformed shaft. Its coordinates in the frame R are (0,y,0). It is interesting to study the translational displacements $u(y,t)$ and $w(y,t)$ of the point C^0 due to bending expressed respectively with respect to the Ox and Oz axes of the frame R.

3. Energy and virtual work computations

The energies are measured from the ground and their terms are written relative to the frame fixed to the support.

3.1. Disk

Since the disk is considered to be rigid, only its kinetic energy T_d is calculated as follows [12]:

$$T_d = \frac{m_d}{2}\left\|\mathbf{v}_{O^l}^{R^g}\right\|^2 + \frac{1}{2}\left(\boldsymbol{\omega}_{R^l}^{R^g}\right)^T \mathbf{I}_{m_d}\boldsymbol{\omega}_{R^l}^{R^g} \quad \text{with} \quad \mathbf{I}_{m_d} = \text{diag}\left[I_{m_d}^{mo} + I_{m_d}^{di} \quad I_{m_d}^{y} \quad I_{m_d}^{mo} - I_{m_d}^{di} \right] \qquad (2)$$

where m_d is the mass of the disk, $\mathbf{v}_{O^l}^{R^g}$ is the translational velocity vector of its center and $\mathbf{I}_{m_d}$ is its principal inertia tensor. $I_{m_d}^{mo}$ and $I_{m_d}^{di}$ are used to distinguish the effects due to the mean inertia of the disk mass and those due to the inertia modeling the disk geometric asymmetry. In addition, $I_{m_d}^{y}$ is the inertia of the disk mass about the Oy axis.

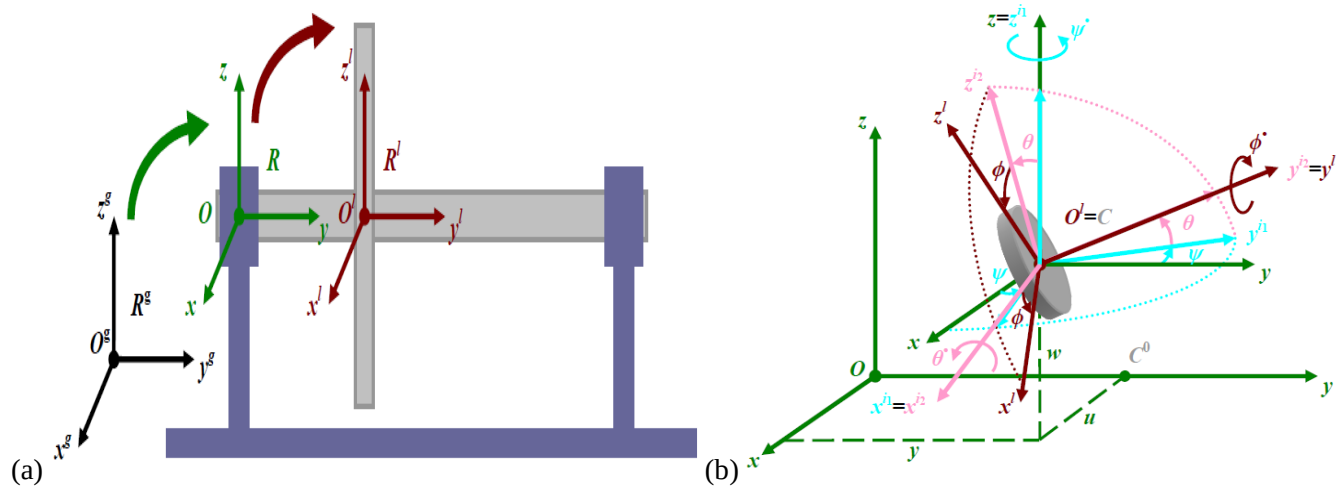

Fig. 1. (a) Frames of reference for the on-board rotor, (b) Euler angles.

The translational velocity vector components $\dot{u}_{O^l}$, $\dot{v}_{O^l}$ and $\dot{w}_{O^l}$ of the disk center are functions of (ω^x,ω^y,ω^z) and (x_O,y_O,z_O). The final expression of the kinetic energy of the disk having a mass center placed at the arbitrary abscissa y_d relative to the frame R is given by [12]:

$$T_d = \frac{m_d}{2}\left(\dot{u}_{O^l}^2 + \dot{v}_{O^l}^2 + \dot{w}_{O^l}^2\right) + \frac{1}{2}\left(I_{m_d}^{mo}\left(\omega^{x^l\,2} + \omega^{z^l\,2}\right) + I_{m_d}^{y}\,\omega^{y^l\,2} + I_{m_d}^{di}\left(\omega^{x^l\,2} - \omega^{z^l\,2}\right)\right) \tag{3}$$

3.2. Shaft

Since the shaft is assumed to be flexible, it is characterized by the kinetic and strain energies and modeled by beam elements. The kinetic energy of a shaft can be obtained by taking a shaft elementary volume which can be considered as a disk of thickness dy. Thus the kinetic energy of a shaft has the following form [12]:

$$T_{sh} = \frac{\rho_{sh} S_{sh}}{2}\int_0^{l_{sh}}\left(\dot{u}_{O^l}^2 + \dot{v}_{O^l}^2 + \dot{w}_{O^l}^2\right)dy + \frac{1}{2}\left(\rho_{sh} I_{S_{sh}}^{mo}\int_0^{l_{sh}}\left(\omega^{x^l\,2} + \omega^{z^l\,2}\right)dy + 2\rho_{sh} I_{S_{sh}}^{mo}\int_0^{l_{sh}}\omega^{y^l\,2}dy + \rho_{sh} I_{S_{sh}}^{di}\int_0^{l_{sh}}\left(\omega^{x^l\,2} - \omega^{z^l\,2}\right)dy\right) \tag{4}$$

where ρ_{sh}, S_{sh} and l_{sh} are respectively the density, the cross-section and the length of the shaft. $I_{S_{sh}}^{mo}$ and $I_{S_{sh}}^{di}$ are respectively the mean inertia of the cross-section and the inertia characterizing the asymmetry of the shaft. The rigid support motion relative to the ground has no influence on the strain energy of the shaft because this energy depends only on the stresses and therefore on the shaft transverse deflection relative to the rotor support R. In addition to the bending deformation, the shear effects highlighted by Timoshenko and the geometric stiffening effects corresponding to the centrifugal stressing due to the support rotations are taken into account. The strain energy of a shaft is given by:

$$\begin{aligned} U_{sh} = {} & \frac{E_{sh} I_{S_{sh}}^{mo}}{2}\int_0^{l_{sh}}\left(\left(\frac{\partial\psi}{\partial y}\right)^2 + \left(\frac{\partial\theta}{\partial y}\right)^2\right)dy + \frac{G_{sh} k_{sh}^{mo} S_{sh}}{2}\int_0^{l_{sh}}\left(\left(\frac{\partial u}{\partial y} + \psi\right)^2 + \left(\frac{\partial w}{\partial y} - \theta\right)^2\right)dy - \frac{1}{2}\left(E_{sh} I_{S_{sh}}^{di}\int_0^{l_{sh}}\left(\left(\frac{\partial\psi}{\partial y}\right)^2 - \left(\frac{\partial\theta}{\partial y}\right)^2\right)dy\right. \\ & \left. - G_{sh} k_{sh}^{di} S_{sh}\int_0^{l_{sh}}\left(\left(\frac{\partial u}{\partial y} + \psi\right)^2 - \left(\frac{\partial w}{\partial y} - \theta\right)^2\right)dy\right)\cos(2\Omega t) - \left(E_{sh} I_{S_{sh}}^{di}\int_0^{l_{sh}}\frac{\partial\psi}{\partial y}\frac{\partial\theta}{\partial y}dy\right. \\ & \left. - G_{sh} k_{sh}^{di} S_{sh}\int_0^{l_{sh}}\left(\frac{\partial u}{\partial y} + \psi\right)\left(\frac{\partial w}{\partial y} - \theta\right)dy\right)\sin(2\Omega t) + \frac{\rho_{sh} S_{sh}}{4}\int_0^{l_{sh}}\left(l_{sh}^2 - y^2\right)\left(\left(\frac{\partial u}{\partial y}\right)^2 + \left(\frac{\partial w}{\partial y}\right)^2\right)dy\left(\omega^{x\,2} + \omega^{z\,2}\right) \end{aligned} \tag{5}$$

where E_{sh} and G_{sh} are respectively the Young's modulus and the shear modulus of the shaft. k_{sh}^{mo} and k_{sh}^{di} are respectively the mean shear coefficient and the shear coefficient relative to the section asymmetry of the shaft.

3.3. Mass unbalance

Let us consider a concentrated mass unbalance m_{mu} positioned at a point P_{mu} of the disk ($y_{mu}=y_d$) with a distance r_{mu} from the shaft geometric center. Its initial angle with the Oz axis of the frame R at rest is η_{mu}. The components of the mass unbalance translational velocity vector $\mathbf{v}_{P_{mu}}^{R^g}$ are functions of (ω^x,ω^y,ω^z) as well as (x_O,y_O,z_O) and are used in the kinetic energy which characterizes the mass unbalance [12]:

$$T_{mu} = \frac{m_{mu}}{2}\left\|\mathbf{v}_{P_{mu}}^{R^g}\right\|^2 \tag{6}$$

3.4. Bearing

Fig. 2a shows a simple diagram of a hydrodynamic bearing which is composed of a fixed journal containing a rotating shaft. The points O and $O^l=C_{sep}$ represent respectively the bearing center and the shaft geometric center. The radius, length and clearance of the bearing are respectively r_{be}, l_{be} and $c_{be}=r_{be}-r_{sh}$ where r_{sh} is the shaft radius. At a constant rotor speed Ω and for a constant static load W_r created by the rotor weight, the shaft center C_{sep} in the bearing holds a static equilibrium position defined by the vector $\boldsymbol{\delta}_{be,sep}=<u_{be,sep},w_{be,sep}>_R^T$ expressed in the frame R or equivalently by the eccentricity $e_{be}=\left\|\boldsymbol{\delta}_{be,sep}\right\|$ of the shaft center in the journal and the attitude angle φ_{be} between the W_r load direction and the line of centers $\mathbf{OC_{sep}}$. In the present study, the short bearing theory is considered ($l_{be}/d_{be}\leq 1/8$ where $d_{be}=2r_{be}$) and the static solution can be obtained using the following formulations deduced from the Reynolds equation with the Gümbel boundary conditions [16]:

$$W_r = \mu r_{be}\left(\frac{r_{be}}{c_{be}}\right)^2\left(\frac{l_{be}}{d_{be}}\right)^2 l_{be}\Omega\frac{\varepsilon_{be}\left(16\varepsilon_{be}^2+\pi^2\left(1-\varepsilon_{be}^2\right)\right)^{\frac{1}{2}}}{\left(1-\varepsilon_{be}^2\right)^2} \quad \text{with} \quad tg\left(\varphi_{be}\right)=\frac{\pi}{4}\frac{\sqrt{1-\varepsilon_{be}^2}}{\varepsilon_{be}} \tag{7}$$

where ε_{be} is the relative eccentricity ($\varepsilon_{be}=e_{be}/c_{be}$) and μ is the fluid film dynamic viscosity. The nonlinear Eq. (7) is solved by an iterative Newton-Raphson method and provides the eccentricity ε_{be} and then the static radial displacement e_{be} of the shaft center. The components of the vector $\boldsymbol{\delta}_{be,sep}$ are obtained by a classical change of basis. The hydrodynamic fluid forces $\mathbf{F}_{be}=<F_{be}{}^u,F_{be}{}^w>_R^T$ produced by the bearings and expressed in the frame R can be obtained by integration of the fluid film pressure (Reynolds equation in the dynamic regime) over the bearing. In order to apply the Lagrange's equations, the virtual work δW_{be} of these forces has to be established:

$$\delta W_{be} = \mathbf{F}_{be}^T\left(\boldsymbol{\delta}_{be},\dot{\boldsymbol{\delta}}_{be}\right)\delta\boldsymbol{\delta}_{be} \tag{8}$$

If the lateral dynamic displacements $\boldsymbol{\delta}_{be}=<u_{be},w_{be}>_R^T$ of the shaft elastic line are assumed to be small in the vicinity of the static position $\boldsymbol{\delta}_{be,sep}$, the linear analysis can be used by constructing a first order Taylor expansion of the fluid film forces $\mathbf{F}_{be}\left(\boldsymbol{\delta}_{be},\dot{\boldsymbol{\delta}}_{be}\right)$ in the vicinity of the static hydrodynamic forces $\mathbf{F}_{be}\left(\boldsymbol{\delta}_{be,sep},\mathbf{0}\right)$ as follows:

$$\mathbf{F}_{be}\left(\boldsymbol{\delta}_{be},\dot{\boldsymbol{\delta}}_{be}\right) = \mathbf{F}_{be}\left(\boldsymbol{\delta}_{be,sep},\mathbf{0}\right) - \mathbf{c}_{be}\boldsymbol{\Lambda}\dot{\boldsymbol{\delta}}_{be} - \mathbf{k}_{be}\boldsymbol{\Lambda}\boldsymbol{\delta}_{be} \tag{9}$$

with

$$\mathbf{c}_{be}=\begin{bmatrix} c_{be}^{xx} & c_{be}^{xz} \\ c_{be}^{zx} & c_{be}^{zz}\end{bmatrix} \quad ; \quad \mathbf{k}_{be}=\begin{bmatrix} k_{be}^{xx} & k_{be}^{xz} \\ k_{be}^{zx} & k_{be}^{zz}\end{bmatrix} \tag{10}$$

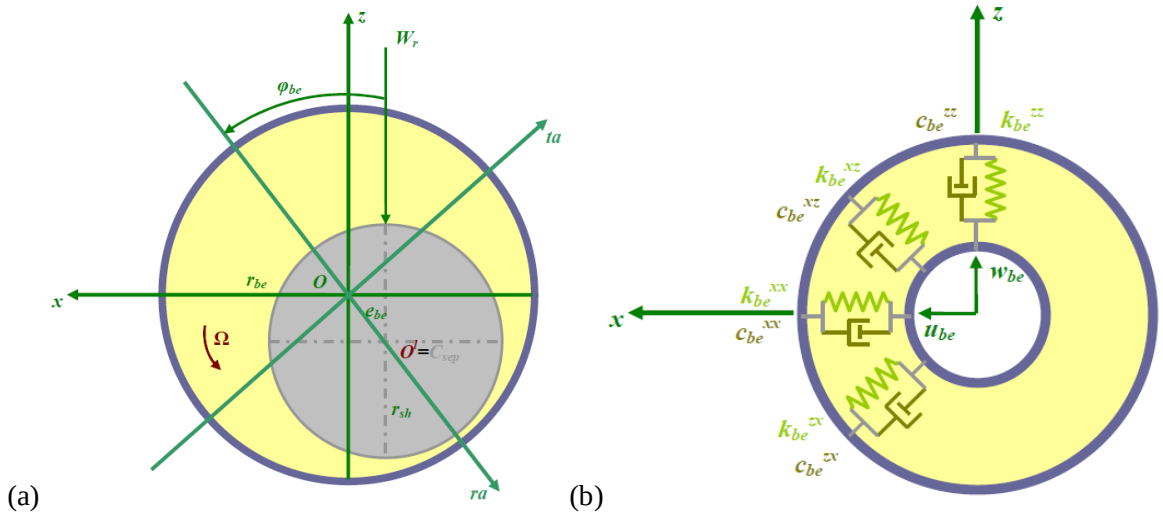

Fig. 2. (a) Sketch of a hydrodynamic bearing, (b) Bearing damping and stiffness coefficients.

and

$$\Delta\boldsymbol{\delta}_{be} = \boldsymbol{\delta}_{be} - \boldsymbol{\delta}_{be,sep} \quad ; \quad \Delta\dot{\boldsymbol{\delta}}_{be} = \dot{\boldsymbol{\delta}}_{be} \tag{11}$$

where $\mathbf{c}_{be}$ and $\mathbf{k}_{be}$ are the damping and stiffness matrices of the linearized hydrodynamic bearing (see Fig. 2b) whose analytical expressions can be found in [16].

4. Equations of motion

The finite element method is chosen for discretizing the rotor and describing its flexural motion as a function of the nodal displacement vector defined by $\boldsymbol{\delta}^n=<u^n,w^n,\theta^n,\psi^n>_R^T$, i.e., the rotor has two translations and two rotations at each node. The finite element used for the shaft modeling has two nodes and the shape functions are based on the Timoshenko beam theory. The linear equations of motion of the finite element rotor model are obtained after applying the Lagrange's equations to the energies for the disk, the shaft finite element and the mass unbalance as well as to the virtual work of the hydrodynamic bearing and assembling appropriately the produced matrices and vectors. They are written with respect to the noninertial reference frame connected to the rotor rigid support *R*:

$$\mathbf{M}_r(t)\ddot{\boldsymbol{\delta}}_r + \mathbf{C}_r(t)\dot{\boldsymbol{\delta}}_r + \mathbf{K}_r(t)\boldsymbol{\delta}_r = \mathbf{F}_r(t) + \mathbf{F}_{be}\left(\boldsymbol{\delta}_{r,sep},\mathbf{0}\right) + \mathbf{K}_{be}\boldsymbol{\delta}_{r,sep} \tag{12}$$

where $\mathbf{M}_r(t)$, $\mathbf{C}_r(t)$ and $\mathbf{K}_r(t)$ are the parametric matrices of mass, damping and stiffness of an asymmetric rotating rotor on moving support. $\ddot{\boldsymbol{\delta}}_r$, $\dot{\boldsymbol{\delta}}_r$ and $\boldsymbol{\delta}_r$ are the acceleration, velocity and displacement vectors of dimension $4(n_{esh}+1)\times 1$ hence n_{esh} is the number of shaft finite elements. $\mathbf{F}_r(t)$ is the external force vector. $\mathbf{F}_{be}(\boldsymbol{\delta}_{r,sep},\mathbf{0})$ is the hydrodynamic force vector caused by the bearing in the static case which opposes the rotor weight $\mathbf{F}_{d,sh}^{W_r}$. In addition, $\boldsymbol{\delta}_{r,sep}$ is the static solution vector of the rotor due to the hydrodynamic bearing.

The matrices of Eq. (12) are expressed in what follows:

$$\begin{aligned}
\mathbf{M}_r(t) &= \mathbf{M}_{d,sh} + \mathbf{M}_{d,sh}^{c_2}\cos(2\Omega t) + \mathbf{M}_{d,sh}^{s_2}\sin(2\Omega t)\\
\mathbf{C}_r(t) &= \mathbf{C}_{be} + \mathbf{C}_{d,sh}^{id} + \mathbf{C}_{d,sh}^{g}\Omega + \mathbf{C}_{d,sh}^{g,c_2}\Omega\cos(2\Omega t) + \mathbf{C}_{d,sh}^{g,s_2}\Omega\sin(2\Omega t) + \mathbf{C}_{d,sh,su}^{re,\omega^y}\omega^y\\
\mathbf{K}_r(t) &= \mathbf{K}_{be} + \mathbf{K}_{sh}^{e} + \mathbf{K}_{sh}^{e,c_2}\cos(2\Omega t) + \mathbf{K}_{sh}^{e,s_2}\sin(2\Omega t) + \mathbf{K}_{d,sh,su}^{re,\dot{\omega}^y}\dot{\omega}^y + \mathbf{K}_{d,sh,su}^{re,\Omega\omega^y}\Omega\omega^y\\
&+\left(\mathbf{K}_{d,sh,su}^{re,\omega^{x2}} + \mathbf{K}_{d,sh,su}^{gse,\omega^{x2}}\right)\omega^{x2} + \mathbf{K}_{d,sh,su}^{re,\omega^{y2}}\omega^{y2} + \left(\mathbf{K}_{d,sh,su}^{re,\omega^{z2}} + \mathbf{K}_{d,sh,su}^{gse,\omega^{z2}}\right)\omega^{z2} + \mathbf{K}_{d,sh,su}^{re,\omega^x\omega^z}\omega^x\omega^z\\
&+\left(\mathbf{K}_{d,sh,su}^{re,\dot{\omega}^y,c_2}\dot{\omega}^y + \mathbf{K}_{d,sh,su}^{re,\Omega\omega^y,c_2}\Omega\omega^y + \mathbf{K}_{d,sh,su}^{re,\omega^{x2},c_2}\omega^{x2} + \mathbf{K}_{d,sh,su}^{re,\omega^{y2},c_2}\omega^{y2} + \mathbf{K}_{d,sh,su}^{re,\omega^{z2},c_2}\omega^{z2} + \mathbf{K}_{d,sh,su}^{re,\omega^x\omega^z,c_2}\omega^x\omega^z\right)\cos(2\Omega t)\\
&+\left(\mathbf{K}_{d,sh,su}^{re,\dot{\omega}^y,s_2}\dot{\omega}^y + \mathbf{K}_{d,sh,su}^{re,\Omega\omega^y,s_2}\Omega\omega^y + \mathbf{K}_{d,sh,su}^{re,\omega^{x2},s_2}\omega^{x2} + \mathbf{K}_{d,sh,su}^{re,\omega^{y2},s_2}\omega^{y2} + \mathbf{K}_{d,sh,su}^{re,\omega^x\omega^z,s_2}\omega^x\omega^z\right)\sin(2\Omega t)
\end{aligned} \tag{13}$$

The subscripts "*d*", "*sh*", "*be*" and "*su*" refer respectively to the disk, shaft, bearing as well as support and express the contribution to the phenomenon represented by the corresponding matrix. The superscripts "c_2" and "s_2" denote the geometric asymmetry of the rotor expressed in terms of the time-varying trigonometric functions $cos(2\Omega t)$ and $sin(2\Omega t)$. The superscript "*id*" stands for the rotor internal damping introduced by estimating the Rayleigh damping coefficients, "*g*" for the rotor gyroscopic effect, "*e*" for the shaft elasticity corresponding to the bending and shear deformations, "*re*" for the rotational effects due to the support rotations (these effects come from the kinetic energies of the disk and the shaft) and "*gse*" for the geometric stiffening effects corresponding to the centrifugal stress due to the support rotations.

The vector $\mathbf{F}_r(t)$ is defined as follows:

$$
\begin{aligned}
\mathbf{F}_r(t) &= \mathbf{F}_{d,sh}^{W_r} + \mathbf{F}_{mu}(t) + \mathbf{F}_{mu,su}(t) + \mathbf{F}_{d,sh,su}(t) + \mathbf{F}_{d,sh,su}^{c_2}(t)cos(2\Omega t) + \mathbf{F}_{d,sh,su}^{s_2}(t)sin(2\Omega t) \\
&= -\mathbf{V}_{d,sh}^{W_r} W_r + \mathbf{V}_{mu}^{c_1}\Omega^2 cos(\Omega t) + \mathbf{V}_{mu}^{s_1}\Omega^2 sin(\Omega t) \\
&+\left(\mathbf{V}_{mu,su}^{\dot\omega^y,c_1}\dot\omega^y + \mathbf{V}_{mu,su}^{\Omega\omega^y,c_1}\Omega\omega^y + \mathbf{V}_{mu,su}^{\omega^{x2},c_1}\omega^{x2} + \mathbf{V}_{mu,su}^{\omega^{y2},c_1}\omega^{y2} + \mathbf{V}_{mu,su}^{\omega^{z2},c_1}\omega^{z2} + \mathbf{V}_{mu,su}^{\omega^x\omega^z,c_1}\omega^x\omega^z\right)cos(\Omega t) \\
&+\left(\mathbf{V}_{mu,su}^{\dot\omega^y,s_1}\dot\omega^y + \mathbf{V}_{mu,su}^{\Omega\omega^y,s_1}\Omega\omega^y + \mathbf{V}_{mu,su}^{\omega^{x2},s_1}\omega^{x2} + \mathbf{V}_{mu,su}^{\omega^{y2},s_1}\omega^{y2} + \mathbf{V}_{mu,su}^{\omega^{z2},s_1}\omega^{z2} + \mathbf{V}_{mu,su}^{\omega^x\omega^z,s_1}\omega^x\omega^z\right)sin(\Omega t) \\
&-\mathbf{V}_{d,sh,su}^{u}\left(\ddot x_O + 2\dot z_O\omega^y - 2\dot y_O\omega^z + z_O\left(\dot\omega^y + \omega^x\omega^z\right) - y_O\left(\dot\omega^z - \omega^x\omega^y\right) - x_O\left(\omega^{y2} + \omega^{z2}\right)\right) \\
&-\mathbf{V}_{d,sh,su}^{w}\left(\ddot z_O + 2\dot y_O\omega^x - 2\dot x_O\omega^y + y_O\left(\dot\omega^x + \omega^y\omega^z\right) - x_O\left(\dot\omega^y - \omega^x\omega^z\right) - z_O\left(\omega^{x2} + \omega^{y2}\right)\right) \\
&-\mathbf{V}_{d,sh,su}^{yw}\left(\dot\omega^x + \omega^y\omega^z\right) + \mathbf{V}_{d,sh,su}^{yu}\left(\dot\omega^z - \omega^x\omega^y\right) - \mathbf{V}_{d,sh,su}^{\theta}\left(\dot\omega^x + \omega^y\omega^z\right) - \mathbf{V}_{d,sh,su}^{\psi}\left(\dot\omega^z - \omega^x\omega^y\right) \\
&-\mathbf{V}_{d,sh,su}^{y\psi}\left(\Omega\omega^x + \omega^x\omega^y\right) + \mathbf{V}_{d,sh,su}^{y\theta}\left(\Omega\omega^z + \omega^y\omega^z\right) - \mathbf{V}_{d,sh,su}^{\theta,c_2}\left(\dot\omega^x - 2\Omega\omega^z - \omega^y\omega^z\right)cos(2\Omega t) \\
&+\mathbf{V}_{d,sh,su}^{\psi,c_2}\left(\dot\omega^z + 2\Omega\omega^x + \omega^x\omega^y\right)cos(2\Omega t) + \mathbf{V}_{d,sh,su}^{\psi,s_2}\left(\dot\omega^x - 2\Omega\omega^z - \omega^y\omega^z\right)sin(2\Omega t) \\
&+\mathbf{V}_{d,sh,su}^{\theta,s_2}\left(\dot\omega^z + 2\Omega\omega^x + \omega^x\omega^y\right)sin(2\Omega t)
\end{aligned}
\qquad (14)
$$

where $\mathbf{V}_{mu}$ ($\mathbf{F}_{mu}(t)$), $\mathbf{V}_{d,sh,su}$ ($\mathbf{F}_{d,sh,su}(t)$) and $\mathbf{V}_{mu,su}$ ($\mathbf{F}_{mu,su}(t)$) are the load vectors (force vectors) associated respectively with the mass unbalance, the inertia force due to support motions and that due to coupling between both phenomena. The superscripts "c_1" and "s_1" signify the components of the mass unbalance force expressed in terms of the time-varying trigonometric functions $cos(\Omega t)$ and $sin(\Omega t)$. The superscripts *u*, *w*, ψ and θ denote the direction of the action force components associated with the rotor support motions.

The transient dynamic motion of the rotor is then obtained by solving Eq. (12) by means of the implicit Newmark scheme based on the average acceleration. The static equilibrium position $\boldsymbol{\delta}_{r,sep}$ is used to initialize the transient dynamic problem. The final integration time is chosen such that the transient effects have disappeared and the steady-state regime has been reached.

5. Results and discussion

The symmetric rotor-rigid/elastic linearized bearing system presented in Fig. 3 is assumed to be subjected to rotating mass unbalance as well as to support harmonic rotation around the *Ox* axis given by $\omega^x=\omega^{x,a}cos(\Omega^x t)$ in rad/s. The physical properties as well as the geometry of the rotor and the bearings are given in Table 1. The shaft is discretized into eight equal length 2-node Timoshenko beam finite elements. The disk is located at node 5 and the bearings # 1 and # 2 are respectively placed at nodes 1 and 9. The rotor is operated at a constant speed of rotation Ω=1200 rpm (20 Hz=mass unbalance frequency). The static equilibrium position of the shaft geometric center in the fluid film bearings is given by $\boldsymbol{\delta}_{be,sep}=<-5.71\times10^{-5},-1.76\times10^{-4}>_R^T$ m. The bearing damping and stiffness matrices are expressed in what follows:

$$
\mathbf{c}_{be} = \begin{bmatrix} 3.50\times10^3 & 1.08\times10^4 \\ 1.08\times10^4 & 7.57\times10^4 \end{bmatrix} \text{N/m/s} \quad ; \quad \mathbf{k}_{be} = \begin{bmatrix} 1.30\times10^6 & 1.32\times10^6 \\ 6.30\times10^6 & 1.94\times10^7 \end{bmatrix} \text{N/m} \qquad (15)
$$

The rotor system is supported either by rigid bearings or hydrodynamic bearings leading in the case of fixed support either to symmetric damping and stiffness matrices with isotropic diagonal and cross-coupling terms or to nonsymmetric matrices respectively.

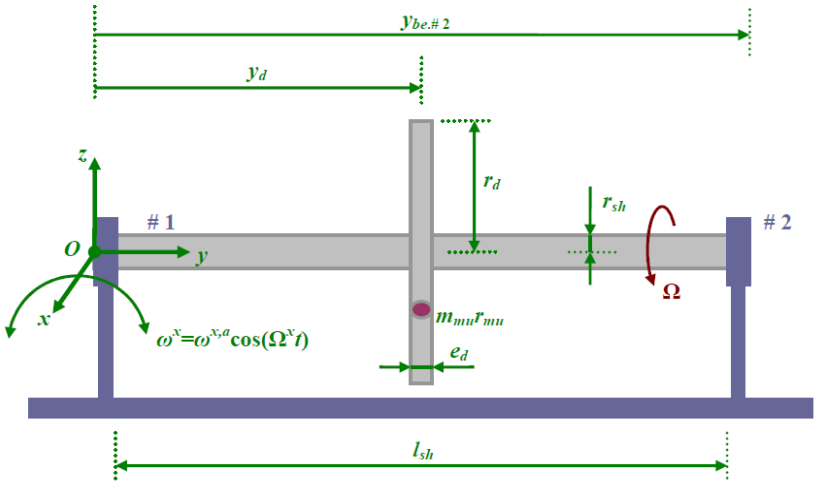

Fig. 3. Description of the on-board rotor system for numerical examples.

Table 1. Details of the investigated rotor system with hydrodynamic bearings

Density of both disk and shaft material	7800 kg/m^3
Radius, thickness and location of the disk	0.15 m, 0.03 m, 0.2 m
shaft material (E_{sh}, ν_{sh})	2×10^{11} N/m^2, 0.3
Radius and length of the shaft	0.04 m, 0.4 m
Mass unbalance	1500 g mm, 0°
Radius and length of the bearings	0.04 m, 0.01 m
Locations of the bearings	0 m, 0.4 m
Radial clearance of the bearings	2×10^{-4} m
Oil film dynamic viscosity	288×10^{-4} Pa s

Fig. 4 shows the classical disk orbit due to the mass unbalance for rigid bearings and a fixed support. Since the matrices of the rotor-bearing system are symmetric and skew-symmetric with isotropic diagonal and cross-coupling components, the dynamic behavior is symmetric and the orbit is circular. Its center coincides with the point O (bearing center). FFT shows that the rotor displacement has an amplitude almost of order 1×10^{-7} m and the same mass unbalance frequency (20 Hz).

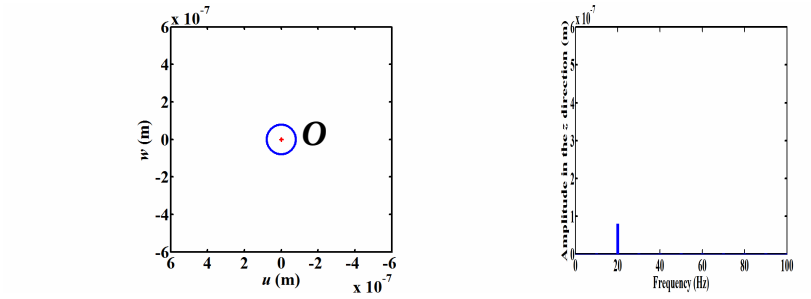

Fig. 4. Mass unbalance orbit and z-FFT of the rotor lateral displacements at the disk for rigid bearings and fixed support.

Fig. 5 gives the disk orbit and FFT of rotor vibrations due to the mass unbalance and the support rotation around the Ox axis. This rotation generates vectors corresponding to force components acting respectively in the Ox

direction (due to the Coriolis acceleration, i.e., the term $-\mathbf{V}_{d,sh,su}^{y\psi}\Omega\omega^{x}$ in Eq. (14)) and in the *Oz* direction (due to the tangential acceleration, i.e., the terms $-\mathbf{V}_{d,sh,su}^{yw}\dot{\omega}^{x}$ and $-\mathbf{V}_{d,sh,su}^{\theta}\dot{\omega}^{x}$ in Eq. (14)). The two transverse displacements associated with these force components are different and this breaks the asymmetry of the rotor behavior. For the selected speed of rotation of the rotor, the *z*-amplitude is very higher than the *x*-amplitude which remains mostly the same. FFT exhibits two frequency components due to the mass unbalance excitation (20 Hz) and to the support harmonic motion (80 Hz).

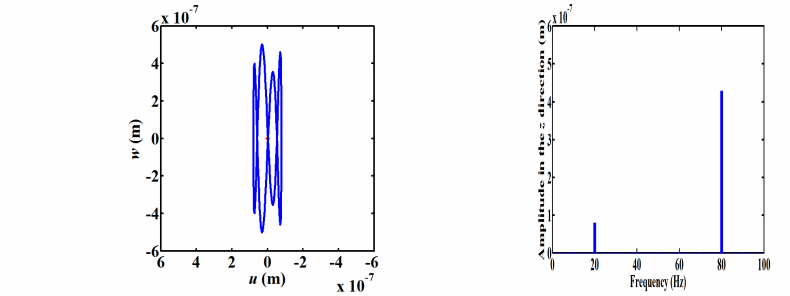

Fig. 5. Disk orbit and *z*-FFT of the flexural vibrations for rigid bearings and a support harmonic rotation: $\omega^{x,a}=5\times10^{-2}$ rad/s and $\Omega^{x}=80$ Hz.

Fig. 6 presents the disk orbit due to the mass unbalance effect in the presence of hydrodynamic bearings. The nonsymmetric damping and stiffness coefficients make the bearings anisotropic and the orbit elliptical with diagonal axes defining the phase between the mass unbalance excitation and the rotor response. The orbit center coincides with the point C_{sep} (static position of the shaft center in the bearings). The orbit is large compared to that corresponding to rigid bearings because of the combination between the bending modes of the rotor and the rigid body modes relative to the rotor motion in the bearings. *z*-FFT indicates that the disk vibration has an amplitude of about 7×10^{-6} m and the same mass unbalance frequency (20 Hz).

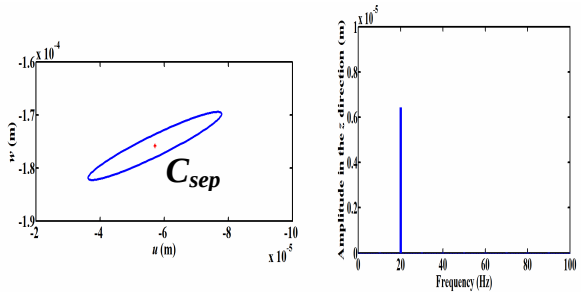

Fig. 6. Mass unbalance orbit and z-FFT of the rotor transverse displacements at the disk for flexible bearings and fixed support.

Fig. 7 displays the disk orbits for hydrodynamic bearings during support rotational motions. The orbit characteristics (shape and magnitude) change with amplitude and frequency of the support harmonic excitation. For very small amplitudes and different frequencies, the orbit shapes become more complicated with respect to those obtained when the support is fixed (see Fig. 7a). It should be noted that the dynamic behavior is all the more modified as the frequency of the support excitation is high compared with the natural frequencies or the speed of rotation of the rotor. On the other hand, the support motion amplitudes change the *x* and *z* orbit magnitudes. FFTs exhibit two frequency components due to the mass unbalance excitation (20 Hz) and to the support harmonic motions (50 Hz and 80 Hz). Even if the support rotations have an influence on the mass unbalance excitation (see Eq. (14)), this influence does not appear clearly in FFTs of the rotor motion during the support harmonic rotation because its amplitude is very small compared to the speed of rotation of the rotor (mass unbalance frequency).

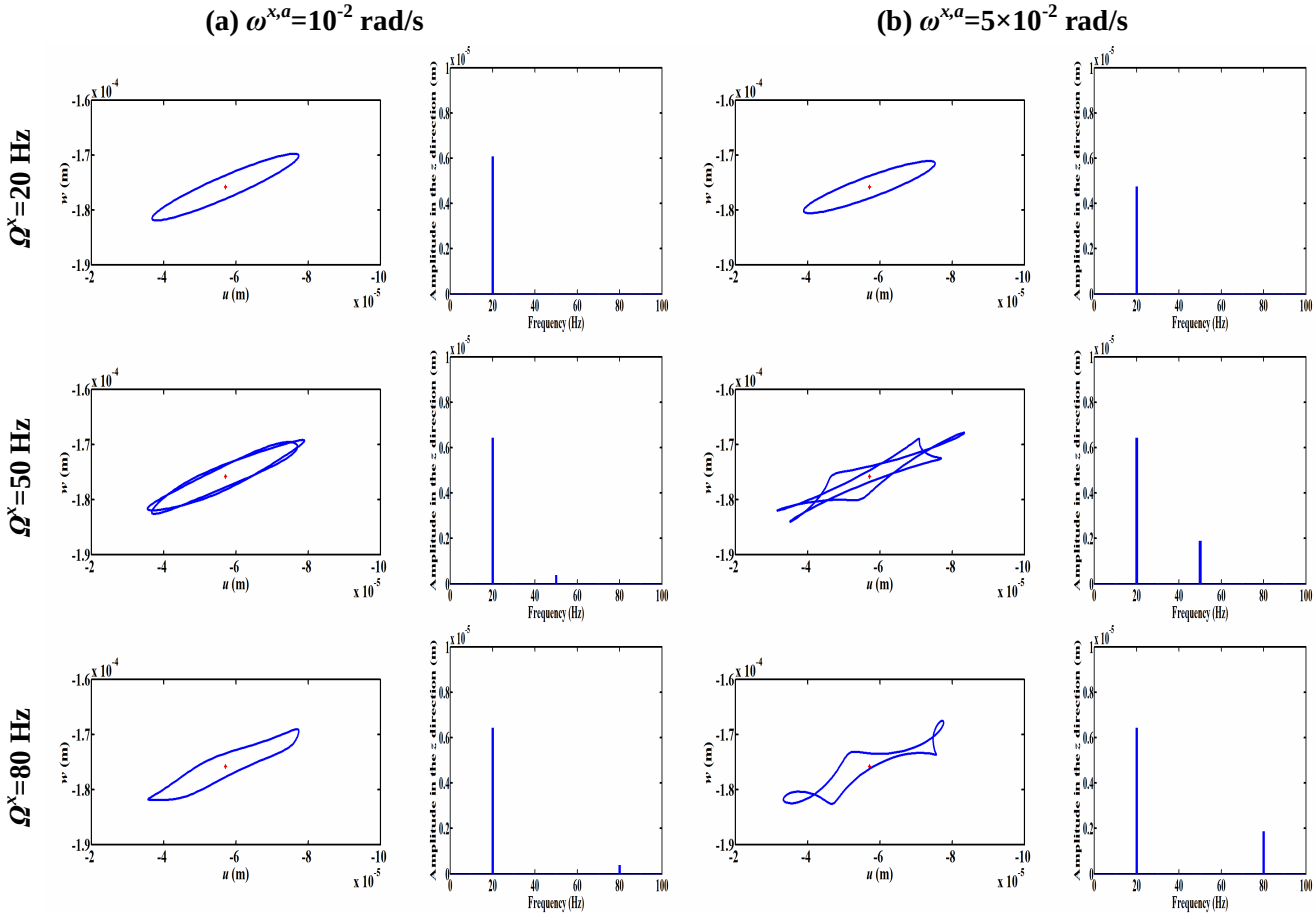

Fig. 7. Disk orbits and z-FFTs of the lateral vibrations for flexible bearings and two amplitudes of support harmonic rotations: $\omega^{x,a}$= (a) 10^{-2} rad/s, (b) 5×10^{-2} rad/s, (Ω^x=20 Hz, 50 Hz AND 80 Hz).

6. Conclusions

A finite element model is presented to analyze the dynamic behavior of a symmetric on-board rotor whose support is subjected to sinusoidal rotation. The rotational effects and the geometric stiffening effects relative to the centrifugal stressing due to the support rotations are taken into account. The support rotations create time-varying parametric coefficients which can lead to lateral dynamic instability. In the case of a rotor mounted on rigid bearings and running at the lower speeds of rotation, the support rotation around a transverse axis creates an orbit having its greatest magnitude in the perpendicular transverse direction. Unlike the previous case, the support rotation effects concern the two transverse directions when the rotor is carried by hydrodynamic bearings. It is noted that the shape and the magnitude of the orbits can be significantly affected by the support motion frequency and amplitude respectively. In the case of considerable rotation amplitude compared to the speed of rotation of the rotor, it is shown that the mass unbalance forces can depend on the support rotation around a transverse axis. The frequency components due to the mass unbalance excitation and to the support harmonic motions appear in FFTs of the rotor flexural vibrations. In the case of large orbits, the assumption of a linearized hydrodynamic bearing model is questionable. A nonlinear model is to be considered and the hydrodynamic bearings have to be treated as external nonlinear forces acting on the shaft.

References

1. M. Lalanne, G. Ferraris, Rotordynamics Prediction in Engineering, Wiley, Chichester, 1998.
2. G. Genta, Dynamics of Rotating Systems, Springer, New York, 2005.
3. R. Dufour, A. Berlioz, Parametric instability of a beam due to axial excitations and to boundary conditions, ASME Journal of Vibration and Acoustics 120 (2) (1998) 461-467.
4. Y. Kang, Y.-P. Shih, A.-C. Lee, Investigation on the steady-state responses of asymmetric rotors, ASME Journal of Vibration and Acoustics 114 (2) (1992) 194-208.
5. V. Srinivasan, A. Soni, Seismic analysis of a rotor-bearing system, Earthquake Engineering and Structural Dynamics 12 (3) (1984) 287-311.
6. Y. Hori, T. Kato, Earthquake-induced instability of a rotor supported by oil film bearings, ASME Journal of Vibration and Acoustics 112 (2) (1990) 160-165.
7. L.E. Suarez, M.P. Singh, M.S. Rohanimanesh, Seismic response of rotating machines, Earthquake Engineering and Structural Dynamics 21 (1) (1992) 21–36.
8. R. Subbiah, R.B. Bhat, T.S. Sankar, Response of rotors subjected to random support excitations, ASME Journal of Vibration, Acoustics, Stress and Reliability in Design 107 (4) (1985) 453-459.
9. A.S. Lee, B.O. Kim, Y.-C. Kim, A finite element transient response analysis method of a rotor-bearing system to base shock excitations using the state-space Newmark scheme and comparisons with experiments, Journal of Sound and Vibration 297 (3-5) (2006) 595-615.
10. F.W. da Silva Tuckmantel, K.L. Cavalca, H.F. de Castro, P. Felscher, R. Markert, An analysis on the supporting structure representative model in rotating systems, Proceedings of the Tenth International Conference on Vibration Problems, Prague, Czech Republic, 5-8 September 2011.
11. N. Feng, E. Hahn, Rotor-model-based identification of foundations in rotating machinery using modal parameters, Proceedings of the Tenth International Conference on Vibration Problems, Prague, Czech Republic, 5-8 September 2011.
12. M. Duchemin, A. Berlioz, G. Ferraris, Dynamic behavior and stability of a rotor under base excitation, ASME Journal of Vibration and Acoustics 128 (5) (2006) 576-585.
13. N. Driot, C.H. Lamarque, A. Berlioz, Theoretical and experimental analysis of a base-excited rotor, ASME Journal of Computational and Nonlinear Dynamics 1 (3) (2006) 257-263.
14. F.M.A. El-Saeidy, F. Sticher, Dynamics of a rigid rotor linear/nonlinear bearings system subject to rotating unbalance and base excitations, Journal of Vibration and Control 16 (3) (2010) 403-438.
15. A.S. Das, J.K. Dutt, K. Ray, Active vibration control of unbalanced flexible rotor-shaft systems parametrically excited due to base motion, Applied Mathematical Modelling 34 (9) (2010) 2353-2369.
16. J. Frêne, D. Nicolas, B. Degueurce, D. Berthe, M. Godet, Hydrodynamic Lubrication Bearings and Thrust Bearings, Elsevier Science, Amsterdam, 1997.